Temperature dependence of the velocity boundary condition for nanoscale fluid flows

Zhaoli Guo, T. S. Zhao,* and Yong Shi
Department of Mechanical Engineering, The Hong Kong University of Science and Technology, Kowloon, Hong Kong
(Received 23 February 2005; revised manuscript received 24 June 2005; published 2 September 2005)

Velocity slips may occur as a fluid flows over a solid surface in the nanometer scale. The slip length L_s, characterizing the degree of slip, is usually used to describe the velocity boundary condition at the fluid/solid interface. In this work, we show that for a given wall-fluid system, the slip length L_s generally varies with the system temperature T. In particular, we show that it is possible to create a pair of solid wall and fluid systems, in which the velocity slip becomes rather small and independent of temperature.

DOI: 10.1103/PhysRevE.72.036301 PACS number(s): 47.11.+j, 61.20.Ja, 83.50.Rp

Although the assumption of the classical no-slip boundary condition works well when the classical hydrodynamic (i.e., the Navier-Stokes) equations are used to model macroscopic flow systems, having a specific boundary condition for fluid flows past a solid surface in the nanometer scale is a critical ingredient for predicting the flow behavior in nanofluidic devices, which are now widespread and finding uses in many scientific and industrial contexts. Both numerical simulations and experimental data have revealed that complicated slip phenomena could occur at the fluid-solid interface, indicating that the mechanics of momentum transfer in the interfacial region is different from that in the bulk flow region. From the molecular point of view, the motion of a fluid molecule near a solid interface is influenced not only by the other neighboring fluid molecules, but also by the neighboring solid molecules, through intermolecular interactions.

The degree of velocity slip can be quantified by the so-called slip length L_s, which is defined as the distance from the wall where the linearly extrapolated tangential velocity matches that of the wall. L_s is actually a reflection of the momentum transfer between the wall and the fluid, and depends on a number of factors. The dependence on the Knudsen number of L_s for dilute gases has been extensively studied since the pioneering work by Maxwell [1]. Studies on the slip phenomena of dense fluids have also been performed recently [2–4]. These studies demonstrate that large velocity slip may also occur at the fluid-solid interface, although the Knudsen number is small, and L_s usually depends on the wettability of the fluid-solid interface in the linear regime where the shear rate $\dot{\gamma}$ is small [5].

It is well understood that the wettability is usually temperature-dependent, and the temperature may also have an influence on the collision frequency between molecules, and thus on the momentum exchange between the fluid and the wall. It is expected that L_s would change with temperature.

The wettability is, in fact, a reflection of the competition between the attractive parts of the fluid-fluid potential and the fluid-wall potential energies. Since the wettability is temperature-dependent, it is expected that L_s would change with temperature. Furthermore, the temperature may also affect the slip length through the repulsive parts of the interaction potentials. A natural question arises then: how does the temperature of the system, or the kinetic energy of the fluid molecules, affect the slippage? Knowledge about this question is of vital importance for dense fluid flows at small scales, as the flow boundary condition that works well at a particular temperature may cause a totally different flow dynamic behavior in a system at a different temperature. Although the influence of temperature on the slippage was mentioned in several previous studies [6], there is as yet no consensus on how temperature affects slip behavior. In this work, we aim to study the temperature dependence of the slip length of a dense fluid in the nanometer scale.

We consider the Couette flow of a dense fluid confined between two parallel walls in the y-z plane, where the fluid molecules interact with a 12-6 Lennard-Jones (LJ) potential, $V(r)=4\varepsilon[(\sigma/r)^{12}-(\sigma/r)^6]$, with ε representing the interaction energy and σ the interaction range. The two walls are located at $x=0$ and $x=H=10\sigma$, respectively, and each exerts a 10-4 potential [7], $V_w(r)=2\pi\epsilon_w[0.4(\sigma/r)^{10}-C(\sigma/r)^4]$. The fluid in the slit is sheared by moving the two walls at $x=0$ and $x=H$ with velocities $-U$ and U in the y direction, respectively.

Such a system is usually studied by employing the molecular-dynamics (MD) or Monte Carlo (MC) simulations, which are rather computationally expensive. Kinetic approach is a possible alternative. It is clear that the Boltzmann theory for a dilute gas is unsuitable for this dense fluid system. The classical Enskog theory for homogeneous dense fluids is also inapplicable since in the nanoscale the molecular size becomes comparable with the system dimension, and the fluid-fluid and fluid-solid interactions become so significant that strong inhomogeneity may be induced. At present, there exist two kinetic theories for dense inhomogeneous fluids [8–10]. Unfortunately, both theories are rather complicated and are difficult to use.

Recently, a simple but robust kinetic model for dense inhomogeneous fluids was proposed by the authors [11]. This kinetic model has been shown to be able to predict both equilibrium and dynamical behaviors of a fluid in the molecular scale that are in *quantitative* agreement with molecular-dynamics and Monte Carlo results. It is expected that the model can be a promising powerful tool for probing the statistic and dynamic behavior of nanoscale fluids. In this

*Corresponding author. Email address: metzhao@ust.hk

work, we use this model to explore the velocity slip behavior at a fluid-solid surface in the nanometer scale.

The kinetic model can be expressed as [11]

$$\partial_t f + \boldsymbol{\xi}\cdot\boldsymbol{\nabla}_{\boldsymbol{r}} f - \frac{1}{m}\boldsymbol{\nabla}_{\boldsymbol{r}}(V_{\text{ext}} + V_m)\cdot\boldsymbol{\nabla}_{\boldsymbol{\xi}} f = \Omega(f), \tag{1}$$

where $f(\boldsymbol{r},\boldsymbol{\xi},t)$ is the single-particle distribution function for molecules with velocity $\boldsymbol{\xi}$ at position $\boldsymbol{r}$ and time t, and m is the molecular mass. $V_{\text{ext}}(\boldsymbol{r}) = V_w(x) + V_w(H-x)$ is the total external potential coming from the two walls; V_m relates to the LJ potential V by $V_m(\boldsymbol{r}) = \int n(\boldsymbol{r}+\boldsymbol{r}')V_{\text{att}}(|\boldsymbol{r}'|)d\boldsymbol{r}'$, where n is the local number density $n = \int f d\boldsymbol{\xi}$, and V_{att} is the long-range attractive part of V, which can be obtained following some systemic methods such as that proposed by Barker and Henderson (BH) [12] or that by Weeks *et al.* (WCA) [13]. The repulsive portion of V, V_{rep}, is simulated by a hard-sphere potential with an effective diameter σ_e, which is represented by the collision operator Ω. In the present study, the LJ potential V is split according to the BH theory, where the effective hard-sphere diameter is approximated by $\sigma_e = \sigma(1+0.2977T^*)/(1+0.33163T^* + 1.04771^{-3}T^{*2})$ with $T^* = k_BT/\varepsilon$ [14]. It is also found that the WCA separation gives results quantitatively similar to those predicted by the BH method. Since the hard-sphere potential in the kinetic model is just an approximation to the repulsive part of the intermolecular potentials, the temperature-dependent diameter σ_e indicates that temperature also affects the latter.

In the kinetic model [11], Ω is further approximated as $\Omega = -\lambda^{-1}[f - f^{(\text{eq})}] + J_{\text{ex}}$, where λ represents a velocity-independent relaxation time, and J_{ex} is given by

$$J_{\text{ex}} = -V_0 f^{(\text{eq})}(\boldsymbol{\xi}-\boldsymbol{u})\cdot[2\boldsymbol{A}\chi^{\text{hs}}(\bar{n}) + \boldsymbol{B}\bar{n}], \tag{2}$$

with $\chi(\bar{n})$ being the radial distribution function (RDF) for a homogeneous hard-sphere fluid of density $\bar{n}$, and $\bar{n} = \int w(\boldsymbol{r}')n(\boldsymbol{r}+\boldsymbol{r}')d\boldsymbol{r}'$ being the average density of n with a weight function $w(\boldsymbol{r})$. In this study, we use the RDF proposed by Carnahan and Sterling [15], $\chi(n) = (1-nV_0/8)/(1-nV_0/4)^3$, and $\bar{n}$ is determined using the Tarazona average method [16]. The two vectors $\boldsymbol{A}$ and $\boldsymbol{B}$ are defined by $\boldsymbol{A}(\boldsymbol{r}) = D^{-1}\int_{|\boldsymbol{r}'|<\sigma/2}\boldsymbol{r}'\bar{n}(\boldsymbol{r}+\boldsymbol{r}')d\boldsymbol{r}'$ and $\boldsymbol{B}(\boldsymbol{r}) = D^{-1}\int_{|\boldsymbol{r}'|<\sigma/2}\boldsymbol{r}'\chi^{\text{hs}}[\bar{n}(\boldsymbol{r}+\boldsymbol{r}')]d\boldsymbol{r}'$, with $D = \pi\sigma^5/120$. $f^{(\text{eq})} = n(2\pi k_BT/m)^{-3/2}\exp[-m(\boldsymbol{\xi}-\boldsymbol{u})^2/2k_BT]$ is the local equilibrium distribution function, where $\boldsymbol{u} = n^{-1}\int \boldsymbol{\xi} f d\boldsymbol{\xi}$ is the fluid velocity. The relaxation time λ in the collision operator is determined based on the local average density model (LADM) [17], i.e., $\lambda(\boldsymbol{r}) = \mu(\bar{n})/nk_BT$, where $\mu(n)$ is the viscosity for a homogeneous dense fluid [18], $\mu(n) = \mu_0 nV_0(Y^{-1} + 0.8 + 0.7614Y)$ with $\mu_0 = (5.0/16\sigma_e^2)\sqrt{k_BT/\pi}$, $Y = nV_0\chi^{\text{hs}}(n)$, and $V_0 = 2\pi\sigma_e^3/3$.

A Chapman-Enskog analysis of the kinetic equation (1) leads to the following equations for the conservative variables n and $\boldsymbol{u}$:

$$\partial_t(mn) + \boldsymbol{\nabla}\cdot(mn\boldsymbol{u}) = 0, \tag{3a}$$

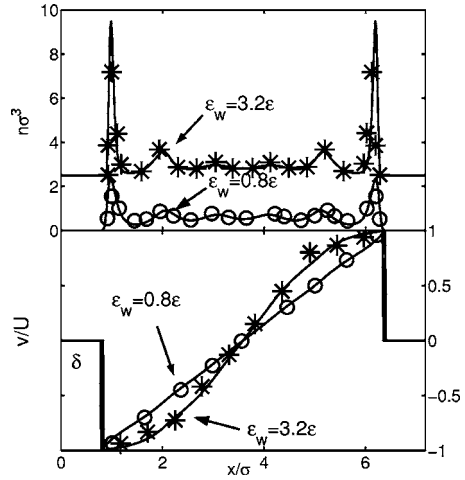

FIG. 1. The density (top) and velocity (bottom) distributions of a Lennard-Jones fluid confined between two 10-4 walls with a separation of $H = 7.178\sigma$. Results are obtained at temperature $T = 1.1\epsilon/k_B$, pore-averaged density $n_0 = \int_0^H n(x)dx/H = 0.519\sigma^{-3}$, and $C = 1.0$. Solid lines are results predicted by the kinetic model [Eq. (3b)], and symbols are the MD results from Ref. [17]. In the top panel, the data for $\epsilon_w = 3.2\epsilon$ are shifted for clarity.

$$\partial_t(mn\boldsymbol{u}) + \boldsymbol{\nabla}\cdot(mn\boldsymbol{u}\boldsymbol{u}) + k_BT\boldsymbol{\nabla}n + n\boldsymbol{\nabla}(V_{\text{ext}} + V_m) = \boldsymbol{\nabla}\cdot[\mu(\bar{n})\overline{\boldsymbol{\nabla}\boldsymbol{u}}] + nk_BT[2\bar{\boldsymbol{A}}\chi^{\text{hs}}(\bar{n}) + \bar{\boldsymbol{B}}\bar{n}]V_0, \tag{3b}$$

where k_B is the Boltzmann constant and $\overline{\boldsymbol{\nabla}\boldsymbol{u}} = [\boldsymbol{\nabla}\boldsymbol{u} + (\boldsymbol{\nabla}\boldsymbol{u})^T]$. It should be recognized that Eq. (3) explicitly includes the effects of the fluid-wall and fluid-fluid interactions and the induced inhomogeneity, whereas these effects are not included in the classical Navier-Stokes equations but are effectively incorporated into the boundary condition.

For the steady planar Couette flow described earlier, the momentum equation (3b) in the x and y directions becomes $d[\ln n + (V_{\text{ext}} + V_m)/k_BT]/dx = -[2A_x\chi(\bar{n}) + B_x\bar{n}]V_0$ and $d[\mu(\bar{n})dv/dx]/dx = 0$, respectively, where v is the velocity component in the y direction. These two equations can be solved numerically to obtain the density and velocity distributions of the Couette flow. The first equation is solved under the condition that the pore-averaged density is a constant, i.e., $n_0 = \int_0^H n(x)dx/H = \text{const}$, and the second equation is solved under the assumption that the fluid molecules in contact with the wall have the same velocity as the wall molecules. Such a treatment is consistent with the analysis done by Koplik *et al.* [19]. In Fig. 1, we compare the results predicted by the kinetic model with the MD results from Ref. [17] with $C = 1.0$ and $\epsilon_w/\epsilon = 3.2$ or 0.8 with $H = 7.178\sigma$. As can be seen, the predicted results are in excellent agreement with those by the MD simulations.

We now use the kinetic model to study the effect of temperature on the flow slippage. We change the interaction parameter C in the wall-fluid potential V_{wf} from 0 to 1 to model a repulsive (nonwetting) or an attractive (wetting) wall. The slip length L_s is determined from the definition $L_s = u_s/\dot{\gamma}$, which reduces to $(2U/\dot{\gamma} - h)/2$ for the Couette flow [5]. Here h is the actual channel width occupied by the fluid, which is usually smaller than H because the fluid molecules can never

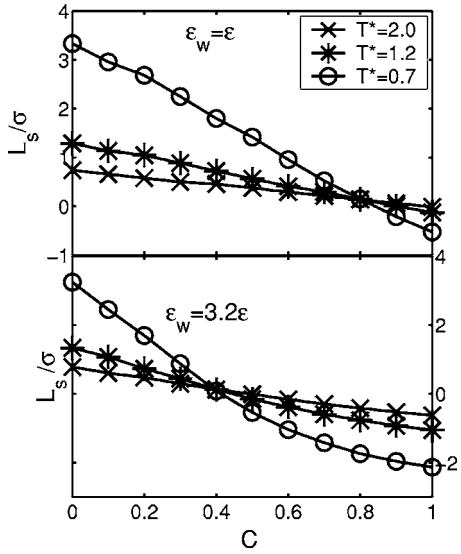

FIG. 2. The slip length (L_s) as a function of the fluid-wall interaction parameter C at different temperatures.

arrive at the wall due to the repulsive force exerted by the wall (see Fig. 1). h is measured as $H-2\delta$, where δ is the distance between the first fluid layer and the wall. In our calculations, δ is determined by looking for the first point x near the wall at which $n(x)>10^{-6}$.

Figure 2 presents the measured slip length L_s as a function of parameter C at three selected temperatures $T^*=k_BT/\epsilon$. As can be seen, large slip always occurs for small values of C, and L_s decreases with increasing C at each temperature. Such a phenomenon was also observed in previous MD studies [2], and was related to the wettability of the wall-fluid system. For a small C, the fluid is nonwetting on the solid surface, and fluid molecules can escape easily from the wall, which will result in a large slippage. On the other hand, as C increases, the wettability of the fluid changes accordingly: a transition from nonwetting to partial wetting and finally to complete wetting may occur. As C becomes sufficiently large, the attractive force of the wall is so strong that the fluid molecules may be trapped by the wall molecules and move with the solid surface. Under such a circumstance, the slippage occurs between the layers of fluid molecules, rather than between the first fluid layer and the wall. Hence, the so-called stick slip can be observed.

We can also observe from Fig. 2 that in general the temperature has a strong influence on the slipping. With the same fluid-wall potential, the magnitude of L_s at a higher temperature is usually smaller than that at a lower temperature. To see this more clearly, we further measured the changes of L_s as T^* ranges from 0.7 to 3.0, for a wall with a weak attractive potential ($C=0.1$) and a wall with a strong attractive potential ($C=1.0$) as $\epsilon_w=3.2\epsilon$. The variation of L_s with temperature T^* at different fluid densities is shown in Fig. 3, which clearly shows temperature affects the slip length: The magnitude of L_s, either for normal slip or stick slip, usually decreases with increasing temperature. Furthermore, it is observed from Fig. 3 that L_s tends to become less dependent on temperature with increasing temperature.

The temperature dependence of the slip length reflects the

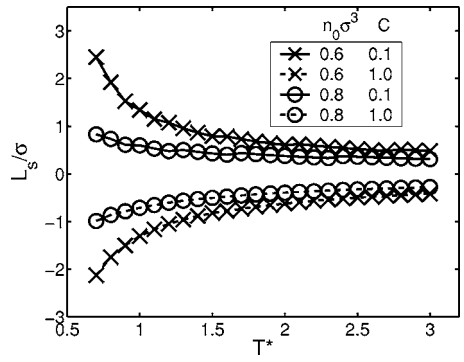

FIG. 3. Slip length as a function of the temperature with different interaction parameter C at different densities ($\epsilon_w=3.2\epsilon$).

competition between the kinetic energy of the fluid molecules and the potential energy of the wall. For a given fluid, the wall potential causes the fluid molecules to form some inhomogeneous structures, while the kinetic energy of the fluid molecules drives them to be uniform. For a wall with a smaller C, the attractive force is weaker and the fluid molecules can escape from the wall easily under the interaction with other fluid molecules. At low temperatures, most of the fluid molecules are inactive and may be accumulated in the central region of the channel, as shown in Fig. 4. Therefore, in such a situation, the momentum transfer between the wall and the fluid will become less efficient and results in a large velocity slip between the fluid and the wall. With an increase in temperature, the fluid molecules becomes more active and some of them in the central region are driven to the region near the wall (see Fig. 4). As a result, the momentum transfer between the wall and the fluid becomes more efficient, and thus the velocity slip between them decreases with increasing temperature. As temperature is sufficiently high, the distribution of the fluid molecules is nearly unaffected by temperature, and at this time the slip length L_s will not change any more with temperature.

The situation for a wall with larger C is quite different. In

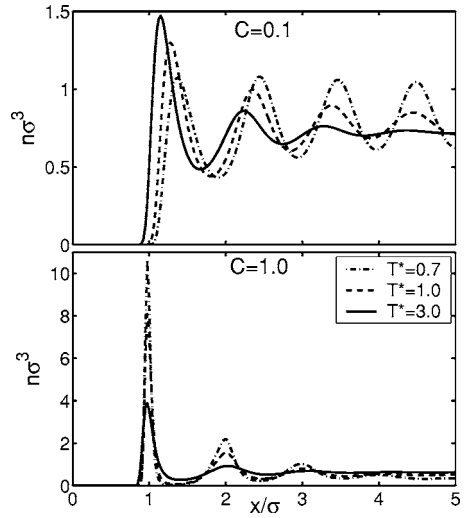

FIG. 4. Density distribution at different temperatures ($\epsilon_w=3.2\epsilon$, $n_0\sigma^3=0.6$).

this case, the attractive force of the wall is so strong that there exists a layer of fluid molecules that stick to and move with the wall, as shown in Fig. 4. The slip under such a situation occurs mainly between the fluid layers rather than the first fluid layer and the wall, and the slip length usually takes negative values. As the temperature increases and the fluid molecules move faster, some of the molecules in the near-wall region will enter the central region (see Fig. 4). As a result, the degree of stick slip becomes weak and $|L_s|$ decreases with increasing temperature.

Another interesting phenomenon is also observed from Fig. 2: For a given fluid density n_0 and a wall-fluid interaction energy ϵ_w, the isothermal lines intersect at the same point, say (C_0, L_{s0}), meaning that as $C=C_0$, the slip length is independent of temperature. Furthermore, it is also noticed that the different ϵ_w results in almost the same L_{s0}. To see this phenomenon more clearly, we present the slip length against temperature with $C=C_0$ in Fig. 5. The magnitude of L_{s0} is of about $0.1-0.2\sigma$, which is much smaller than the channel size. This means that in such a particular pair of solid wall and fluid systems, the classical nonslip boundary condition can be used.

We also find that C_0 depends on the energy ϵ_w for a given n_0 following a power law as

$$C_0 \sim \epsilon_w^{-3/5}. \tag{4}$$

To see the physical meaning of Eq. (4), we rewrite the 10-4 wall-fluid potential $V_w(r)$ as $V_w(r)=2\pi\epsilon_w'[0.4(\sigma'/r)^{10}-(\sigma'/r)^4]$, where $\sigma'=\sigma C^{-1/6}$ and $\epsilon_w'=\epsilon_w C^{5/3}$. Therefore, when $C=C_0$, the wall-fluid potential will have the same rescaled interaction energy ϵ_w'. We wish to point out that this interesting phenomenon is also observed for other values of n_0 and ϵ_w, and thus we speculate that it may be a peculiar phenomenon in nanofluidics.

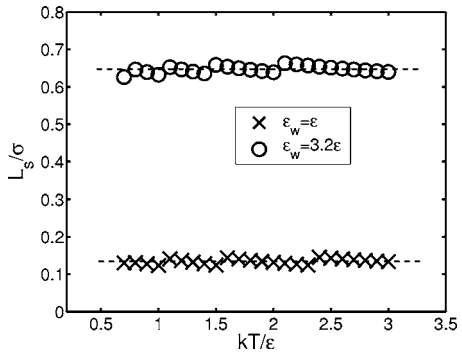

FIG. 5. The slip length against the temperature as $C=C_0$. The data for $\epsilon_w=3.2\epsilon$ are shifted upward by 0.5σ for clarity in the bottom panel. The dashed lines are a guide for the eye.

In summary, we find that temperature has a complicated influence on the velocity slip behavior as a dense fluid flows over a solid wall in the nanometer scale. For a given fluid, if the wall has a weak attractive energy, the fluid velocity undergoes a normal slip, while if attractive energy is strong, the fluid velocity usually undergoes a stick slip. The degree of both kinds of slip generally decreases with increasing the system temperature. Yet there exist some systems consisting of a particular pair of solid and fluid in which the slip becomes independent of temperature.

The support from an RGC grant of Hong Kong (Grant No. HKUST6197/03E) is gratefully acknowledged. The authors thank Dr. Chao Xu for helpful discussions.

[1] J. C. Maxwell, Philos. Trans. R. Soc. London **170**, 231 (1867).
[2] J.-L. Barrat and L. Bocquet, Phys. Rev. Lett. **82**, 4671 (1999); Faraday Discuss. **112**, 119 (1999).
[3] Y. Zhu and S. Granick, Phys. Rev. Lett. **87**, 096105 (2001).
[4] J. S. Ellis, G. McHale, G. L. Hayward, and M. Thompson, J. Appl. Phys. **94**, 6201 (2003).
[5] P. A. Tompson and S. M. Troian, Nature (London) **389**, 360 (1997). In this work it was observed that at high shear rate, large slip can appear even at a wetting wall and the slip length strongly depends on the shear rate nonlinearly. In the present work, we focus on the case of small shear rate.
[6] U. Heinbuch and J. Fischer, Phys. Rev. A **40**, 1144 (1989); P. A. Thompson and M. O. Robbins, *ibid.* **41**, 6830 (1990).
[7] W. A. Steele, Surf. Sci. **36**, 317 (1973).
[8] H. T. Davis, J. Chem. Phys. **86**, 1474 (1987); Chem. Eng. Commun. **58**, 413 (1987).
[9] H. T. Davis, I. Bitsanis, T. K. Vanderlick, and M. V. Tirrell, in *Supercomputer Research in Chemistry and Chemical Engineering*, ACS Symposium Series 353, edited by K. S. Jensen and D. G. Truhlar (ACS, Washington, D.C., 1987); H. T. Davis, *Fundamentals of Inhomogeneous Fluids*, edited by D. Henderson (Marcel Dekker, New York, 1992).
[10] L. A. Pozhar and K. E. Gubbins, J. Chem. Phys. **94**, 1367 (1991); **99**, 8970 (1993); L. A. Pozhar, *Transport Theory of Inhomogeneous Fluids* (World Scientific, Singapore, 1994).
[11] Z. Guo, T. S. Zhao, and Y. Shi, Phys. Rev. E **71**, 035301(R) (2005).
[12] J. A. Barker and D. Henderson, J. Chem. Phys. **47**, 4714 (1967); Rev. Mod. Phys. **48**, 587 (1976).
[13] J. D. Weeks, D. Chandler, and H. C. Andersen, J. Chem. Phys. **54**, 5237 (1971).
[14] R. L. Cotterman, B. J. Schwarz, and K. E. Prausnitz, AIChE J. **32**, 1787 (1986); Y. Tang, J. Chem. Phys. **116**, 6694 (2002).
[15] N. F. Carnahan and K. E. Starling, J. Chem. Phys. **51**, 635 (1969); **53**, 600 (1970).
[16] P. Tarazona, Phys. Rev. A **31**, 2672 (1985).
[17] I. Bitsanis, J. J. Magda, M. Tirrell, and H. T. Davis, J. Chem. Phys. **87**, 1733 (1987).
[18] J. W. Dufty, A. Santos, and J. J. Brey, Phys. Rev. Lett. **77**, 1270 (1996); A. Santos, J. M. Montanero, J. W. Dufty, and J. J. Brey, Phys. Rev. E **57**, 1644 (1998).
[19] J. Koplik, J. R. Banavar, and J. F. Willemsen, Phys. Fluids A **1**, 781 (1989).